05,06,13

Influence of the Elastically Stressed State of Interfaces on the Magnetoelectric Properties of Ferromagnetic/Ferroelectric Layered Structures

© S.A. Sharko[1], A.I. Serokurova[1], N.N. Novitskii[1], N.N. Poddubnaya[2], V.A. Ketsko[3], A.I. Stognij[1]

[1] Scientific and Practical Materials Research Center, National Academy of Sciences of Belarus, Minsk, Belarus
[2] Institute of Technical Acoustics, National Academy of Sciences of Belarus, Vitebsk, Belarus
[3] Kurnakov Institute of General and Inorganic Chemistry, Russian Academy of Sciences, Moscow, Russia

E-mail: sharko@physics.by

Received April 17, 2023
Revised April 17, 2023
Accepted May 11, 2023

In the layered ferromagnetic/ferroelectric structures in the form of cobalt, nickel or permendur layer on a ferroelectric substrate of lead zirconate titanate obtained by ion-beam sputtering — deposition, relative strains due to mismatch of crystal lattices of mating materials at the metal/substrate in-terface make a more noticeable contribution to the magnetoelectric response than those associated both with the magnetostriction of the ferromagnetic layer and with the piezoelectric effect of the ferroelectric substrate. The structures obtained are characterized by the thermal stability and reproducibility of magnetoelectric characteristics and can be used as converters of magnetic and electrical quantities, for example, in magnetic field sensors and actuators.

Keywords: Ion beam sputtering — deposition, ion beam planarization, ferromagnetic/ferroelectric interface, layered structures, magnetoelectric effect.

DOI: 10.21883/PSS.2023.06.56110.27H

1. Introduction

Materials science has achieved tremendous success in development of new (functional) materials over the last decades. This is mainly due to the increasing demand for materials with unique properties for various research, development and business applications. To a large extent, this includes such materials whose properties may be controlled in a wide range through external electric and magnetic fields.

Fundamental relationship between electrical and magnetic properties of matter in condensed state is detected using a magnetoelectric (ME) effect [1–3]. This phenomenon is based on interaction between electric and magnetic ordered subsystems through a mechanical coupling: mechanical strain induced by an external impact on one of the subsystems (electric or magnetic) causes an appropriate response in the other subsystem. Impact of the magnetic subsystem on the electric system is referred to as a direct ME effect [4], if the magnetic state in the external electric field is changed — this is the inverse effect [5]. ME effect is observed most distinctly in layered composite structures where both ordered subsystems are separated from each other in space. Such structures are a particular case of a more general class — multiferroic materials [1–3] — composite materials whose structure has at least two of three ordering: electric, magnetic and mechanical. In such materials, ME effect is a new property which is not known for their components (multiplicativity).

Materials based on the ME effect [6] may used as various magnetic and electrical transducers. This is, for example, non-volatile MeRAM [7] and high-sensitive magnetic field sensors [8–10]. Composite systems in the form of layered ferromagnetic/ferroelectric structures [6,7,11,12] have much higher ME effect at room temperature [3,10] than single-phase materials [3,13,14]. Multiferroic materials in the form of layers of ferromagnetic (FM) metals and their alloys on zirconate-based ferroelectric (FE) ceramic substrates — lead titanate (PZT) are of great interest. PZT-based solid solutions have high residual polarization, piezoelectric modulus and mechanical quality factor [15,16].

Most of the currently existing methods for formation of layered composite structures is based on mechanical bonding of ferroelectric and ferromagnetic layers, for example, by adhesion [3,14,17,18]. These methods allow to achieve high ME performance [3]. However, these methods, though good as they may be, are unsuitable either for thermostable materials with reproducible properties, which is important for operation of devices at high temperatures; or for ME effect investigation in a limiting transition to low thicknesses. All these features arise from the presence of an adhesive layer at the ferromagnetic/ferroelectric interface, which intrinsically reduces the direct interaction between

components at low frequencies that are much lower than the typical mechanical vibration excitation frequencies.

The ion-beam sputtering — deposition method [19–22] allows to prevent these disadvantages by directly applying an FM metal layer to the FE substrate after ion-beam planarization of the surface and to provide direct metallic layer/substrate contact. This allows to form a thermostable plane-parallel interface and produce layered ferromagnetic/ferroelectric structures with ME effect [23] at room temperature. On the other hand, production of thin layers from both FM and FE components provokes interest in the investigation of ME effect during limiting transition to low thicknesses and interfaces. In particular, the role of interface in formation of ME properties shall grow with decreasing FM layer thickness. This is equivalent to the increasing contribution of elastic strain in FM and FE components at the interface.

This study uses the ion-beam sputtering — deposition method to produce structures in the form of $2\,\mu$m cobalt, nickel and permendur FM layers on $400\,\mu$m PZT FE ceramic substrates — $PbZr_{0.45}Ti_{0.55}O_3$. Prevailing influence of elastic stress state at the ferromagnetic/ferroelectric interface on formation of low-frequency ME effect is shown compared with FM layer magnetostriction and FE substrate piezoeffect.

2. Experiment

$PbZr_{0.45}Ti_{0.55}O_3$ FE ceramics was synthesized in the form of pellets 8 mm in diameter and $400\,\mu$m in thickness using a standard solid-phase synthesis method [19] by sintering powder-like PbO, ZrO_2 and TiO_2 taken in the appropriate proportion and pressed at $2 \cdot 10^8$ Pa. The ceramic substrate surface was gradually treated by mechanochemical polishing and ion-beam planarization methods to achieve a nanoscale rms roughness level.

The ion-beam planarization consisted of two stages. At the first stage, a $0.2\,\mu$m planarization PZT layer was deposited on the initial PZT substrate surface by target sputtering during 45 min with 1.2–1.4 keV oxygen ions. At the second stage, the substrate surface with the deposited layer was subjected to 0.4 keV oxygen ion sputtering to a depth twice as large as the planarizing layer thickness. Ion-beam planarization of the ceramic substrate surface reduces typical projections and depressions and completely removes small surface irregularities. Then the planarized ceramic substrate surface was coated with a FM metal layer deposited at a rate of $1.1\,\mu$m/h by ion-beam sputtering a cobalt, nickel or permendur target with 1.4 keV argon ions. Permendur (Pdr) is a solid solution of cobalt (49%), iron (49%) and vanadium (2%) [24].

The samples were polarized in 4 kV/mm DC electric field during two h at 150°C using the procedure described in [25]. magnetoelectric measurements were performed at room temperature in persistent and alternating magnetic fields at 1 kHz using the procedure described in [26]. The magnetic field was applied along the sample surface and the electric field was excited perpendicular to it (transverse ME effect geometry). For thermostability study, the planarized substrate structure samples were uniformly cooled down and heated in the range from −25 to +120°C during five 2 h cycles [19].

X-ray examinations of the obtained heterostructures were carried out using Bruker D8 Advance (Germany, 2013) diffractometer in the range of 2θ 20–60° with 1.5405 Å Cu–K_α radiation. The phases were identified using the Inorganic crystal structure database [27]. Cross-sections of the obtained heterostructures were analyzed using FEI Company (USA) Helios NanoLab 600SEM microscope. Cross-sections were obtained by 32 keV focused gallium ion beams. Metal layer thicknesses were measured using MII-4 Linnik–Nomarski interference microscope and SEM data.

3. Results and discussion

The developed surface of the ceramic samples makes some problems associated with achievement of high quality continuous metal layers with a thermostable plane-parallel metal/substrate interface even after standard mechanochemical treatment. The surface consists of a disordered crystallite assembly with random orientation (Figure 1, *a*) and mean size of projections and depressions in the same scale as the crystallite mean size ($\sim 1\,\mu$m).

The metal layer surface of Co ($3\,\mu$m)/PZT ($400\,\mu$m) structure obtained by cobalt layer deposition on the PZT substrate (Figure 1, *b*) after ion-beam planarization has clearly visible defects in the form of depressions and individual projections with a typical size of $\sim 1\,\mu$m that are inherited from the substrate surface. The latter are easily removed by means of surface planarization by the PZT oxygen ion beam O^+. There are irregular cavities inside the substrate itself which are formed both during ceramic substrate synthesis with loose interfacing of crystal grains and during formation of a structure cross-section by focused Ga^+ beam resulting in precipitation of individual

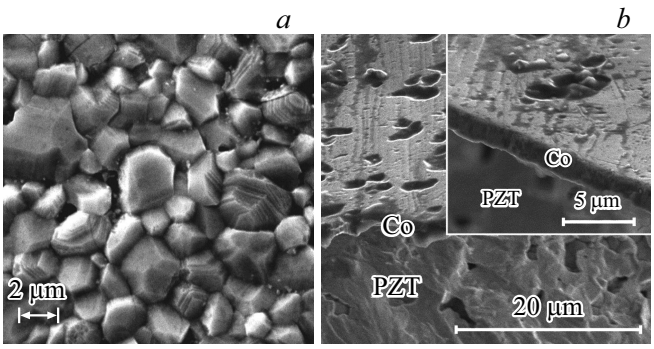

Figure 1. Cross-section of the initial ceramic sample obtained using SEM (*a*), cross-section and Co ($3\,\mu$m)/PZT ($400\,\mu$m) heterostructure surface with polished PZT substrate (*b*), cobalt layer on the substrate with high magnification (right top detail).

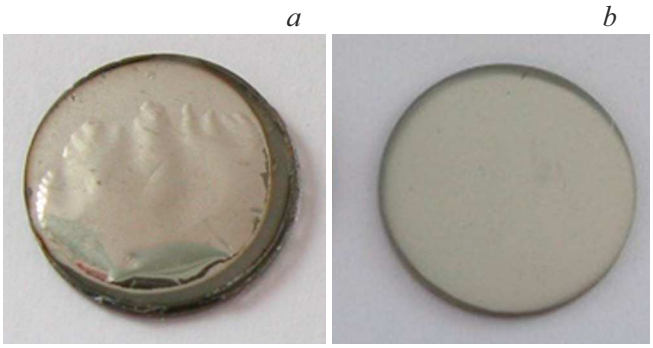

Figure 2. View of Co/PZT samples after thermal cycling in the range from −25 to +120°C before (*a*) and after (*b*) ion-beam planarization of PZT substrate surface.

grains. On the planarized substrate surface, the metal forms a continuous layer that conformally follows the large surface irregularities (Figure 1, *b*, right top detail).

In case of developed substrate surface profile, the metal film is exposed to bending stresses. In case of thermal impacts, they grow considerably, in particular in sharp-angled interface points due to the difference in the thermal expansion coefficients of the metal film and PZT substrate. Insufficient heat removal in this points causes degradation of the initial samples (Figure 2, *a*) exposed to thermal impacts. When a metal layer is deposited on a planarized surface, adhesion between the metal layer and substrate is increased. consequently, the interface becomes flat, parallel and smooth. In this case, the metal film is exposed to tensile and compressive stresses only, and the layered structure exposed to thermal impact is not damaged and retains its appearance (Figure 2, *b*).

X-ray images (Figure 3) of layered Co/PZT, Ni/PZT and Pdr/PZT structures on planarized substrates have all main FE substrate reflections and most intensive FM metal layer reflections. Their angular displacements $\Delta\theta$ with respect of equilibrium positions are indicative of stressed condition of the interface areas both in the metal layer on the substrate and in the substrate itself [22,28]. Relative modifications of interplanar spacing $\Delta d/d$ perpendicular to the sample surface

$$\Delta d/d = -\operatorname{ctg}\theta\Delta\theta, \qquad (1)$$

account for less than 1% and only rarely exceed 2% (Table 1). The „minus“ sign correspond to compressive strain and emerging tensile stresses.

According the accommodation model [29,30] applied to epitaxial ferrite-garnet films, stressed region thickness is determined by the lattice mismatch of the metal film and substrate

$$f^{\max} = \Delta a/a = (a_{\text{sub}} - a_{\text{film}})/a_{\text{film}}, \qquad (2)$$

where a_{sub} and a_{film} are substrate and metal layer lattice constants in stressed state at room temperature along the interface. At sufficiently low f equal to f^{sprin} ($\sim 10^{-3}$ [30]), the epitaxial layer is elastically strained up to the equality of tangential lattice constants of the metal layer and substrate (along the interface). When applying this model to the continuous plane-parallel Me/PZT interface, as in this case, it should be taken into account that the epitaxial growth of metal layers is possible only in individual areas consisting of single-crystal grain surfaces (quasi-epitaxial growth). There-

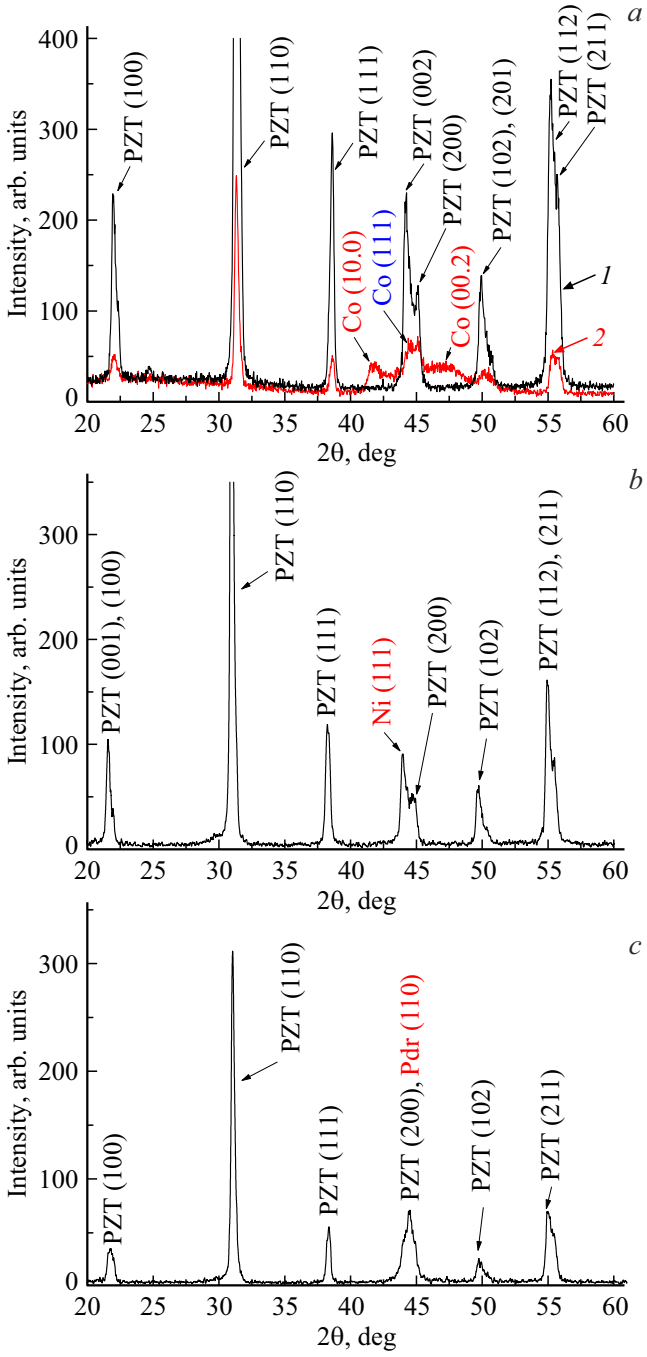

Figure 3. X-ray image of planarized PZT substrate (*1*) and Co/PZT (*2*) (*a*), Ni/PZT (*b*), Pdr/PZT structures (*c*). Pdr — permendur. Thicknesses of all metal layers are 2 μm, substrate thickness is 400 μm.

Table 1. Diffraction reflection angles 2θ-from the cobalt, nickel and permendur layers and PZT substrate obtained from the X-ray images (Figure 3), relative interplanar spacing distortions $\Delta d/d$ calculated using equation (1), and relative strain ε of the film and substrate perpendicular to the interface and caused by the interplanar spacing distortions, and calculated using equation (4)

	Reflection	2θ, deg.		$\Delta d/d$	ε, 10^{-6}
		X-ray image, 2θ	Tabular value, $2\theta_{tab}$		
Co	10.0	41.56	41.6	0.0009	0.25
	111	44.38	44.2	−0.004	−35
	00.2	47.26	47.3	0.0008	3.5
PZT	100	21.94	22.1	0.007	1.7
	110	31.33	31.0	−0.01	−2.4
	111	38.62	38.4	−0.005	−1.2
Ni	111	43.99	44.60	0.013	160
PZT	100	21.63	22.1	0.021	2.5
	110	30.99	31.0	0.0003	0.36
	111	38.27	38.41	0.004	4.8
Pdr	110	44.51	44.83	0.007	30
PZT	100	21.63	22.1	0.021	1.1
	110	30.99	31.0	0.0003	0.15
	111	38.27	38.41	0.004	2.0

fore, in these conditions, epitaxy may be treated with a certain degree of conditionality. PZT ceramics has a tetragonal lattice with $a = 4.017$ Å and $c = 4.139$ Å [16,31]. Cobalt has a hexagonal close-packed structure with $a = 2.505$ Å and $c = 4.089$ Å [32], nickel and permendur crystallize in a FCC lattice with 3.524 Å [33] and 2.857 Å [27], respectively. Lattice mismatch f (Table 2) is much higher than the elastic relaxation of mechanical stresses f^{sprin}, therefore, to explain the fracture resistance of metal films, mechanism of internal stress relaxation on mismatch dislocations shall be taken into account.

Minimum thickness of the metal or substrate transition layer, where full stress relaxation takes place, equal to

$$h_{\min} = (f^{\max}/f^{\text{sprin}})d_0, \tag{3}$$

where d_0 is the lattice constant of the metal layer or substrate perpendicular to the surface, accounts for the thousandth — tenth of a micrometer (Table 2).

Mean tangential strain values at the metal/substrate interface

$$\varepsilon = \nu \frac{(\Delta d/d)}{2h_{\min}} d_0, \tag{4}$$

where ν is Poison's ratio for the metal layer or substrate, d_0 is the same parameter as in (3), are about $10^{-7}-10^{-5}$ (Table 1). In some cases, strain in the metal layer is much higher than the corresponding strain in the substrate. Poison's ratio is associated with mutual orthogonality of interplanar spacing strain Δd and lattice constants Δa. For all metals (including cobalt, nickel, and permendur), this is within $0.3-0.4$ [34], and for PZT — this is within $0.28-0.32$ [35, p. 268].

Dependences of linear transverse ME stress coefficient α of the studied structures produced on the planarized PZT ceramic substrates on the persistent magnetic field are shown in Figure 4. The equation describing the electric response in heterogeneous, in particular, layered structures with ME interaction is written as (with linear approximation in the effective medium model [3,23]):

$$\mathbf{D} = e\mathbf{S} + \varepsilon\mathbf{E} + \alpha\mathbf{H}, \tag{5}$$

where $\mathbf{D}$ is the electric induction, $\mathbf{S}$ is the strain, $\mathbf{E}$ is the electric field strength, $\mathbf{H}$ is the magnetic field strength; e is the piezoelectric coefficient, ε is the dielectric constant, α is the ME coefficient.

Without an external electric field as it follows from equation (5), the electric response is determined by elastic mechanical impact through piezoelectric and ME coefficients, respectively. ME coefficient α is a product of piezoelectric and piezomagnetic moduli [3,23]. The latter is defined as a coefficient of the linear term of the magnetostriction expansion as a power series in the magnetic field strength. Magnetostriction coefficients for permendur in the corresponding magnetic fields are an order of magnitude higher than those of less strictional materials such as cobalt and nickel [36,37]. However, as shown in Figure 4, ME coefficient α for it is much lower. On the other hand, the maximum mismatch of the interfaced lattices is higher for Co/PZT structure (Table 2), and the ME effect is higher, respectively (Figure 4, a). This suggests a greater role of elastic stress state at the layer interface, rather than FM layer magnetostriction at low frequencies of the alternating magnetic field. Actually, as shown above (Table 2), the relative contribution of the elastic-stress region of the FM layer to the ME effect determined by the ratio of region thickness $h_{\min}$ and metal layer thickness, with various

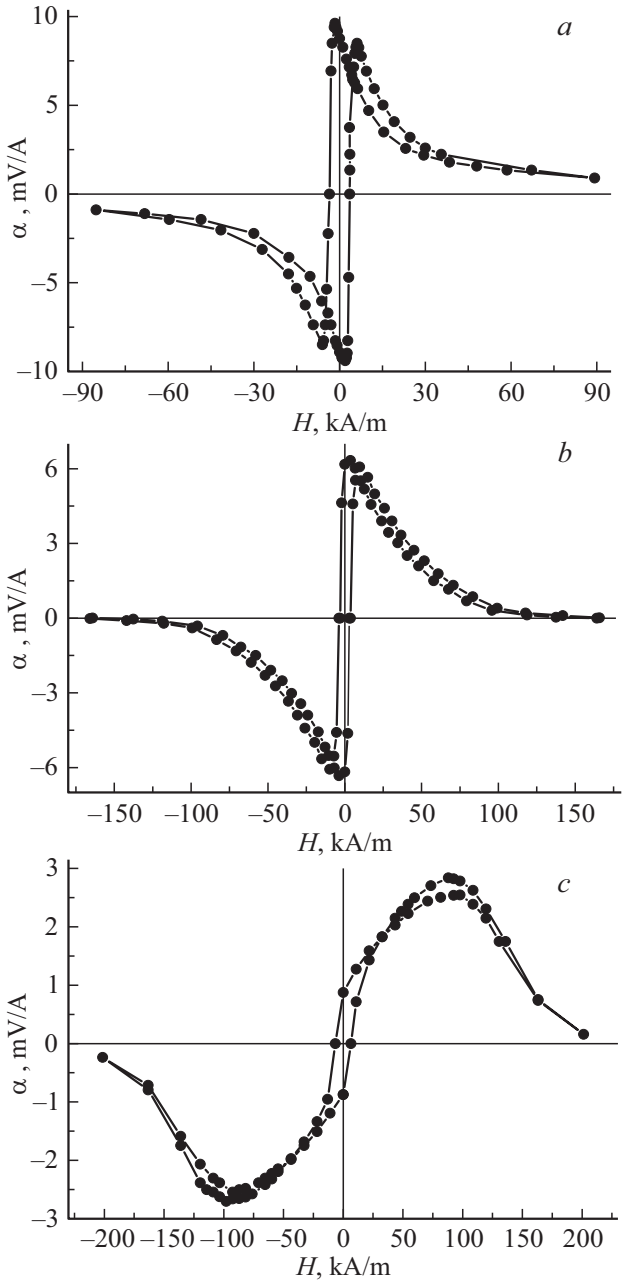

Figure 4. ME-properties of heterostructures Co/PZT (*a*), Ni/PZT (*b*) and Pdr/PZT (*c*) in the external magnetic field in transverse configuration. Pdr — permendur. Thicknesses of all metal layers are 2 μm, substrate thickness is 400 μm.

combinations of FM metal and substrate lattice constants is within the range from 0.001 to 0.3.

Relative strain induced in an unattached sample due to the ME effect, in the most general terms without taking into account the anisotropic nature (in this case all indices are omitted), may be estimated using equation

$$\varepsilon = dE = d\alpha H, \tag{6}$$

where d is the piezoelectric modulus; α is the ME stress coefficient; E and H are electric and magnetic field strengths, respectively. piezoelectric coefficients d_{31} and d_{33}, respectively, are equal to −93.5 and 223 pC/N [35, p. 136].

Table 2. The maximum ME stress coefficient α; magnetic field H, where the maximum is achieved as shown in Figure 4; magnetostriction coefficient λ [36,37] in this field H; minimum $(\Delta a/a)_{\min}$ and maximum $(\Delta a/a)_{\max}$ lattice mismatch of FM layer and FE substrate calculated using equation (2); minimum FM layer thicknesses $h_{\min}$ corresponding to $\Delta a/a$ and calculated using equation (3); relative strain ε induced by the inverse piezoelectric effect and calculated using equation (6); as well as ratio of magnetostriction energy W_λ and elastic strain energy W_ε of the FM layer

	ferromagnetic layer		
	Co	Ni	Pdr
α, mV/A	8.5	6.3	2.8
H, kA/m	6.1	3.8	88
λ	$-3 \cdot 10^{-6}$	$-8 \cdot 10^{-6}$	$8 \cdot 10^{-5}$
$(\Delta a/a)_{\min}$	0.012	0.14	0.406
$h_{\min}$, μm	0.003	0.050	0.12
$(\Delta a/a)_{\max}$	0.652	0.175	0.449
$h_{\min}$, μm	0.27	0.062	0.13
ε, 10^{-9}	5.2	6.2	25
W_λ/W_ε	$\sim 10^{-10}$	$\sim 10^{-7}$	$\sim 10^{-6}$

Calculation using equation (6) for the structures with Co, Ni and Pdr yields the relative substrate strain values about 10^{-9}–10^{-8} (Table 2), i. e. they are at least two orders of magnitude lower that the strain in the metal film and substrate caused by lattice mismatch at the interface (Table 1). This fact supports our interface ME effect concept put forward earlier in [19–22,28,38,39], according to which a considerable contribution to the ME interaction is made by the ferromagnetic/ferroelectric interface. This is due to direct interaction between FM and FE components ensured by strong adhesion between the film and substrate. As has been already mentioned beffore, this is possible in layered composite structures produced by ion-beam sputtering–deposition when intermediate meduim in the form of adhesive binding is avoided [3,17,18].

To compare contributions from magnetostriction and elastic stress state at the interface, energy of strain induced for all three obtained structures with cobalt, nickel and permendur may be roughly estimated. Elastic strain energy caused by magnetostriction W_λ and by lattice mismatch W_ε is proportional to the square of the corresponding relative strain

$$W_\lambda = \frac{E\lambda_s^2}{2} V_\lambda, \quad W_\varepsilon = \frac{E}{2}\left(\frac{\Delta a}{a}\right)^2 V_\varepsilon, \tag{7}$$

where E is the Young's modulus for isotropic medium, V_λ is the ferromagnetic volume, λ_s is the magnetostriction coefficient equal to the relative longitidinal strain of a ferromagnet in the magnetic field, V_ε is the volume of the metallic layer region in elastic stress state. Comparing expressions (7), it can be seen that $W_\lambda/W_\varepsilon \propto [\lambda_s/(\Delta a/a)]^2$,

i. e. the elastic strain energy in the interface region is several orders of magnitude higher than the magnetostriction energy of the FM layer (Table 2).

It should be noted that the estimates of the relative contribution of the stress state at the interface and of magnetostriction to the general energy balance are rather conditional. The metal layer on the polycrystalline substrate is also polycrystalline. Therefore, the internal stresses are caused not only by the stress at the interface due to the lattice and thermal expansion coefficient mismatch of the materials in direct contact, but also by crystallite disordering throughout the ceramic substrate depth. Stresses induced by lattice mismatch quickly relax to the metal layer thickness lower than one micrometer, while other stresses associated with crystallite disordering are present in the whole metal layer and grow with its thickness.

4. Conclusion

The ion-beam sputtering — deposition method provides layered structures in the form of $2\,\mu$m cobalt, nickel and permendur layers on planarized ferroelectric ceramic substrates based on lead zirconate titanate — $PbZr_{0.45}Ti_{0.55}O_3$. The produced structures have low-frequency magnetoelectric effect at room temperature. The maximum magnetoelectric effect at an alternating magnetic field frequency of 1 kHz is 8.5 mV/A for structures with cobalt, 6.3 mV/A for structures with nickel and 2.8 mV/A for structures with permendur.

It is shown that elastic strain at the interface regions make a larger contribution to the formation of magnetoelectric properties than magnetostriction of the ferromagnetic layer. Mechanical strain analysis shows that the strain induced by lattice mismatch at the film/substrate interface are at least two orders of magnitude higher that the substrate strain induced by the inverse piezoeffect due to magnetoelectric interaction. The latter supports the interface magnetoelectric effect in the obtained structures.

These structures are characterized by high thermal stability in the range from -25C to $+120^{\circ}$C, repeatability of magnetoelectric properties and are suitable for applications as sensor elements for permanent magnetic field detectors requiring no standby power supply and operated at domestic power supply frequencies.

Acknowledgments

The authors are grateful to Yu. Radyusha (SPC NAS of Belarus in materials science) for the assistance in X-ray examinations.

Funding

The study was supported by grant of the Russian Science Foundation No. 23-43-10004 and Belarusian Republican Foundation for Fundamental Research T23RNF-010.

Conflict of interest

The authors declare that they have no conflict of interest.

References

[1] N.A. Spaldin. Proc. Roy. Soc. A **476**, 0542 (2020).
[2] N.A. Spaldin, R. Ramesh. Nature **18**, *3*, 203 (2019).
[3] C.-W. Nan, M.I. Bichurin, S. Dong, D. Viehland, G. Srinivasan. J. Appl. Phys. **103**, 031101 (2008).
[4] G.-L. Yu, H.-W. Zhang, F.-M. Bai, Y.-X. Li, J. Li. Comp. Struct. **119**, 738 (2015).
[5] P. Zhou, M.A. Popov, Y. Liu, R. Bidthanapally, D.A. Filippov, T. Zhang, Y. Qi, P.J. Shah, B.M. Howe, M.E. McConney, Y. Luo, G. Sreenivasulu, G. Srinivasan, M.R. Page. Phys. Rev. Mater. **3**, 044403 (2019).
[6] A.P. Pyatakov, A.K. Zvezdin. Phys. Usp. **55**, 557 (2012).
[7] A.T. Chen, Y.G. Zhao. APL Mater. **4**, 032303 (2016).
[8] E. Yarar, S. Salzer, V. Hrkac, A. Piorra, M. Höft, R. Knöchel, L. Kienle, E. Quand. Appl. Phys. Lett. **109**, 022901 (2016).
[9] J. Lenz, A.S. Edelstein. IEEE Sens. J. **6**, *3*, 631 (2006).
[10] Y. Wang, J. Li, D. Viehland. Mater. Today **17**, *6*, 269 (2014).
[11] K.-H. Cho, Y. Yan, C. Folgar, S. Priya. Appl. Phys. Lett. **104**, 222901 (2014).
[12] D.A. Filippov, T.A. Galichyan, V.M. Laletin. Appl. Phys. A **116**, *4*, 2167 (2014).
[13] S. Dong, J.-F. Li, D. Viehland. IEEE Ultrason. Ferr. **50**, 1236 (2003).
[14] G. Srinivasan, E. Rasmussen, J. Gallegos, R. Srinivasan, Yu.I. Bokhan, V.I. Laletin. Phys. Rev. B **64**, 214408 (2001).
[15] M. Klee, R. Eusemann, R. Waser, W. Brand, H. Van Hal. J. Appl. Phys. **72**, 1566 (1992).
[16] N. Izyumskaya, Y.-I. Alivov, S.-J. Cho, H. Morkoç, H. Lee, Y.-S. Kang. Curr. Opin. Solid State Mater. Sci. **32**, 111 (2007).
[17] G. Srinivasan, Y.K. Fetisov, L.Y. Fetisov. Appl. Phys. Lett. **94**, 132507 (2009).
[18] L.Y. Fetisov, D.V. Chashin, Y.K. Fetisov, A.G. Segalla, G. Srinivasan. J. Appl. Phys. **112**, 014103 (2012).
[19] A.I. Stognij, N.N. Novitskii, S.A. Sharko, A.V. Bespalov, O.L. Golikova, V.A. Ketsko. Inorg. Mater. **48**, *8*, 832 (2012).
[20] A. Stognij, N. Novitskii, A. Sazanovich, N. Poddubnaya, S. Sharko, V. Mikhailov, V. Nizhankovski, V. Dyakonov, H. Szymczak. Eur. Phys. J. Appl. Phys. **63**, 21301 (2013).
[21] A. Stognij, N. Novitskii, N. Poddubnaya, S. Sharko, V. Ketsko, V. Mikhailov, V. Dyakonov, H. Szymczak. Eur. Phys. J. Appl. Phys. **69**, 11301 (2015).
[22] A.I. Stognij, S.A. Sharko, A.I. Serokurova, S.V. Trukhanov, A.V. Trukhanov, L.V. Panina, V.A. Ketsko, V.P. Dyakonov, H. Szymczak, D.A. Vinnik, S.A. Gudkova, N.N. Poddubnaya, C. Singh, Y. Yang. Ceram. Int. **45**, *10*, 13030 (2019).
[23] M.I. Bichurin, V.M. Petrov, G. Srinivasan. J. Appl. Phys. **92**, *12*, 7681 (2002).
[24] E.P. Wohlfarth. Ferromagnetic materials. A handbook on the properties of magnetically ordered substances. Elsevier (1999). V. 2. P. 168–170.
[25] A.I. Stognij, N.N. Novitskii, S.A. Sharko, A.V. Bespalov, O.L. Golikova, A. Sazanovich, V. Dyakonov, H. Szymczak, V.A. Ketsko. Inorg. Mater. **50**, *3*, 275 (2014).
[26] V.M. Petrov, G. Srinivasan, V.M. Laletin, M.I. Bichurin, D.S. Tuskov, N.N. Poddubnaya. Phys. Rev. B **75**, 174422 (2007).

[27] International Centre for Diffraction Data. (1998). JCPDS.
[28] A.I. Stognij, N.N. Novitskii, S.V. Trukhanov, A.V. Trukhanov, L.V. Panina, S.A. Sharko, A.I. Serokurova, N.N. Poddubnaya, V.A. Ketsko, V.P. Dyakonov, H. Szymczak, C. Singh, Y. Yang, J. Magn. Magn. Mater. **485**, 291 (2019).
[29] J.W. Matthews, S. Mader, T.B. Light. J. Appl. Phys. **41**, 3800 (1970).
[30] A.M. Prokhorov, G.A. Smolenskii, A.N. Ageev. Sov. Phys. Usp. **27**, 339 (1984).
[31] Landolt-Bornstein. Numerical data and functional relationships in science and technology. Group III. Crystal Solid State Phys. V. 4(b). Magnetic and Other Properties of Oxides / Eds K.-H. Hellwege, A.M. Hellwege. Springer-Verlag, N.Y. (1970).
[32] C. Kittel. Introduction to Solid State Physics. John Wiley & Sons. Inc. Berkeley (1996). 408 p.
[33] J. Emsley. The Elements. Oxford University Press. (1998). 300 p.
[34] I.S. Grigoriev, E.Z. Meilikhov, A.A. Radzig. Handbook of Physical Quantities. CRC Press (1996). 1568 p.
[35] B. Yaffe, W. Cook, G. Yaffe. Piezoelektricheskaya keramika /Pod red. L.A. Shuvalova. Mir, M., (1974). 288 p. (in Russian).
[36] Y. He, J.-P. Wang. IJICS **6**, *2/3*, 1 (2016).
[37] The free dictionary https://encyclopedia2.thefreedictionary.com/Magnetostrictive+effect, 2021 (accessed 14 February 2023).
[38] S.A. Sharko, A.I. Serokurova, N.N. Novitskii, N.N. Poddubnaya, V.A. Ketsko, A.I. Stognij Ceram. Int. **48**, *9*, 12387 (2022).
[39] S.A. Sharko, A.I. Serokurova, N.N. Novitskii, V.A. Ketsko, A.I. Stognij. Ceram. Int. **46**, *14*, 22049 (2020).

Translated by Ego Translating